Fast Simulation of Analog Circuit Blocks under Nonstationary Operating Conditions

(Article begins on next page)

07 May 2024

Fast Simulation of Analog Circuit Blocks under Nonstationary Operating Conditions

Tommaso Bradde, *Graduate Student Member, IEEE*, Stefano Grivet-Talocia, *Fellow, IEEE*, Pedro Toledo, *Graduate Student Member, IEEE* Anton V. Proskurnikov, *Senior Member, IEEE*, Alessandro Zanco, *Graduate Student Member, IEEE* Giuseppe C. Calafiore, *Fellow, IEEE*, Paolo Crovetti *Senior Member, IEEE*

Abstract—This paper proposes a black-box behavioral modeling framework for analog circuit blocks operating under small-signal conditions around non-stationary operating points. Such variations may be induced either by changes in the loading conditions or by event-driven updates of the operating point for system performance optimization, e.g., to reduce power consumption. An extension of existing data-driven parameterized reduced-order modeling techniques is proposed that considers the time-varying bias components of the port signals as non-stationary parameters. These components are extracted at runtime by a lowpass filter and used to instantaneously update the matrices of the reduced-order state-space model realized as a SPICE netlist. Our main result is a formal proof of quadratic stability of such Linear Parameter Varying (LPV) models, enabled by imposing a specific model structure and representing the transfer function in a basis of positive functions whose elements constitute a partition of unity. The proposed quadratic stability conditions are easily enforced through a finite set of small-size Linear Matrix Inequalities (LMI), used as constraints during model construction. Numerical results on various circuit blocks including voltage regulators confirm that our approach not only ensures the model stability, but also provides speedup in runtime up to 2 orders of magnitude with respect to full transistor-level circuits.

Index Terms—Behavioral models, Parameterized models, Linearized models, Small-signal analysis, LPV models, Asymptotic stability, Quadratic stability, Lyapunov functions, Voltage regulators.

I. INTRODUCTION

In the last decades, the technological development of compact and portable electronic systems has shown a constantly increasing trend, that is expected to be maintained in the near future. The need for miniaturized, powerful and cost-effective electronics has been boosted by the demand for ubiquitous and interconnected devices, which forces the designers to meet conflicting goals in terms of performance, reliability and power consumption [1]. From an engineering perspective, this scenario requires the development of complex Systems-on-Chip (SoC) or Systems-in-Package (SiP) in which digital, radio frequency components (RF) and analog circuit blocks (CB) operate at very low power supply levels, within the same compact volume. Under the electrical performance standpoint, this interaction translates into the presence of non-negligible coupling and interference parasitic effects, that can lead to

Dept. Electronics and Telecommunications, Politecnico di Torino, Torino 10129, Italy (e-mail: tommaso.bradde@polito.it, stefano.grivet@polito.it, pedro.toledo@polito.it, anton.p.1982@ieee.org, alessandro.zanco@polito.it, giuseppe.calafiore@polito.it, paolo.crovetti@polito.it).

severe signal and power integrity issues; on the other hand, from a functional perspective, the device may be required to work under a variety of operational modes, which can change dynamically according to event-based conditions triggered by the components interaction.

The above facts imply that testing and optimization of such electronic systems cannot be performed considering the single components as stand-alone units, since their interactions determine the overall device functioning. Thus, whenever a prototype design is available, the electrical performance verification is necessarily carried out through transient simulations, in which a highly detailed description of the whole system is considered. Unfortunately, the overwhelming complexity of such simulations, combined with the need for considering phenomena that take place on very broad ranges of time scales, may lead to unaffordable execution time requirements, limiting the possibility of extensively testing and optimization.

In this view, reduced order behavioral models represent a valuable alternative to native components descriptions, as they allow for drastic reduction of the simulation complexity. While the derivation of reduced order models is somehow an established practice for what concerns the linear passive components entering the system (see e.g. [2], [3], [4]), obtaining the same kind of simplified descriptions for non-linear elements is still an open research field.

Modeling frameworks that have been proposed to approximate generic nonlinear circuit blocks include the classical Hammerstein-Wiener model structure identification [5], trajectory piecewise linear approaches [6], Volterra series based methods [7], X Parameters [8], and neural networks [9], [10]. All of these identification methods are characterized by specific drawbacks and advantages in terms of model complexity, accuracy and generation time requirements. This implies that the most appropriate modeling strategy is to be chosen with respect to the application of interest, based on the characteristics of the reference circuit.

In this work, we focus on a class of non-linear circuit blocks deliberately designed to operate as linearly as possible around a prescribed operating point. These circuits will be denoted henceforth as *mildly nonlinear*. Ubiquitous examples of such circuits are Low-Noise Amplifiers (LNA), Operational Amplifiers (OPA), or Low DropOut (LDO) voltage regulators. We explicitly exclude circuits whose behavior relies on strong nonlinearities, such as mixers, phase locked loops, nonlinear oscillators or frequency dividers. When mildly-nonlinear

circuits are properly designed, their behavior in correspondence of a fixed bias condition can be safely approximated by linearized dynamics. As small-signal analysis is often sufficient to validate the proper functioning of these circuits around a prescribed bias condition, affine linearized models of reduced order have been proposed in the past to replace the original circuit description for system level simulations [11]. These models guarantee a drastic reduction of the description complexity and high accuracy whenever the small-signal conditions are met. Additionally, due to their linear nature, they ensure that fundamental physical properties, such as stability, can be guaranteed by construction. A complete energetic characterization of the affine linearized models has been also provided in our recent works [12], [13].

This work proposes an extension to the standard Linear Time-Invariant (LTI) affine linearized models from [14], by admitting non-stationary bias conditions. Taking advantage of a suitable formulation based on a Linear Parameter Varying (LPV) model structure, we show that the proposed reduced-order models are able to accurately approximate the port signals of a transistor-level circuit block when the operating point changes in time. Such changes may be induced by variations in the loading conditions or system-driven events for performance optimization, e.g. reducing power consumption.

The proposed LPV model is constructed from frequency-domain samples of multiple small-signal responses corresponding to a set of static bias levels in a given design range. Using a standard rational fitting process based on the Parametrized Sanathanan-Koerner (PSK) iteration [15], a multivariate rational approximation is constructed, which is then cast in a state-space (descriptor) form or an equivalent SPICE netlist, where all model coefficients or netlist components are found (in closed form) as functions of the bias level. Non-stationary bias conditions are then embedded in the model using a feed-through term resulting from a low-pass filtering operation on the port signals. This operation is performed at run-time and its computational cost is negligible.

Our main technical contribution is related to asymptotic stability of the resulting models. By making use of Lyapunov theory, we are in fact able to prove a property which is stronger than the quadratic stability [16], and entails the asymptotic stability under any possible time-varying bias conditions within their design range. This proof is enabled by a specific choice of basis functions defining model parameterization, which must constitute a positive partition of unity. As a result, quadratic stability is attained by enforcing a finite number of small-size Linear Matrix Inequality (LMI) conditions on the model coefficients during its identification.

The proposed modeling framework is then applied to two examples of LDO voltage regulators with different parameterization schemes. The results confirm the excellent accuracy with respect to transistor-level description, the major speedup, and an experimental verification of the quadratic stability conditions embedded in the model structure.

This work is organized as follows. Section II provides some general background and introduces notation. Section III states the main problem that is addressed, defining applicability limits, and presenting the general proposed LPV model structure.

Section IV discusses stability and provides our formal proof, deriving the stability constraints that should be enforced during model identification. Section V describes the low-pass filtering process for the extraction of time-varying bias conditions. Finally, Section VI presents various numerical examples.

II. BACKGROUND AND NOTATION

We consider a mildly nonlinear analog circuit block accessible from P electrical interface ports. The circuit dynamics are described by the following differential equations

$$
\begin{aligned}
\dot{\xi}(t) &= F(\xi(t), u(t)), \\
\eta(t) &= G(\xi(t), u(t)),
\end{aligned}
\tag{1}
$$

where $u(t), \eta(t) \in \mathbb{R}^P$ denote system input and output signals, $\xi(t) \in \mathbb{R}^N$ is the system state vector and F, G are nonlinear differentiable maps. The state space representation (1) is general and may represent a full transistor-level circuit, possibly including dynamic parasitic effects from a post-layout extraction. Thus, the system dimension N can be very large, and the closed-form representations of maps F, G can be either unavailable (being e.g. encoded by the circuit netlist, which is encrypted and/or provided by third parties) or impractical due to the excessive complexity.

A. Affine Linearized Models

Whenever the circuit block operates under small-signal conditions, affine linearized models of reduced order can be considered as good candidates to replace the reference circuit equations [11], [14]. More precisely, the signals involved in (1) can be decomposed according to

$$
u(t) = U_0 + \tilde{u}(t), \quad \xi(t) = \Xi_0 + \tilde{\xi}(t), \quad \eta(t) = Y_0 + \tilde{\eta}(t), \tag{2}
$$

where the quantities $\tilde{u}(t)$, $\tilde{\eta}(t)$ and $\tilde{\xi}(t)$ are small deviations from a stable working point, identified by the triple of constant vectors (U_0, Ξ_0, Y_0) that satisfy the DC steady-state conditions

$$
\begin{aligned}
0 &= F(\Xi_0, U_0), \\
Y_0 &= G(\Xi_0, U_0).
\end{aligned}
\tag{3}
$$

In compliance with most transient circuit simulation environments, we will assume that for the reference starting time $t = 0$ all the small signals components in (2) are null, and that the circuit operating point is initialized according to (3).

The objective of an affine linearized model is to provide a compact approximate description for the circuit input-output relationship $U_0 + \tilde{u}(t) \rightarrow Y_0 + \tilde{\eta}(t)$, which can replace (1) in order to speed up a transient simulation. Such model can be derived through a sequence of steps, discussed below.

A formal derivation of the small signal transfer function from $\tilde{u}(t)$ to $\tilde{\eta}(t)$ is obtained by linearizing (1) around the equilibrium (3)

$$
\tilde{\mathsf{H}}(s) = \tilde{D} + \tilde{C}(sI_N - \tilde{A})^{-1}\tilde{B}, \tag{4}
$$

where

$$
\begin{aligned}
\tilde{A} &= F'_{\Xi}(\Xi_0, U_0) & \tilde{B} &= F'_U(\Xi_0, U_0) \\
\tilde{C} &= G'_{\Xi}(\Xi_0, U_0) & \tilde{D} &= G'_U(\Xi_0, U_0)
\end{aligned}
\tag{5}
$$

are the matrices of partial derivatives of maps F, G and I_N is the identity matrix of size N. Since we do not assume these maps to be available, a data-driven approach is used to estimate $\tilde{H}(s)$. First, a set of samples $\tilde{H}_k = \tilde{H}(j\omega_k)$ is computed at a discrete set of frequencies ω_k by means of an AC sweep performed within the SPICE solver where the circuit description is available. Then, a low order rational approximation $H(s) \approx \tilde{H}(s)$ is obtained through a fitting process. This approximation task can be performed by standard algorithms in the Loewner Matrix [17] or Vector Fitting [18] frameworks, which allow to cast $H(s)$ into a state space form

$$\begin{aligned}\dot{\tilde{x}}(t) &= A\tilde{x}(t) + B\tilde{u}(t), \quad \tilde{x}(0) = 0 \\ \tilde{y}(t) &= C\tilde{x}(t) + D\tilde{u}(t),\end{aligned} \quad (6)$$

with $\tilde{x} \in \mathbb{R}^n$ and $n \ll N$.

The system (6) provides only a prediction for the small signal components and cannot be used as a direct replacement of (1). An *affine linearized model* [12] is defined as an augmented version of (6), as

$$\begin{aligned}\dot{x}(t) &= Ax(t) + Bu(t), \quad x(0) = X_0 \\ y(t) &= Cx(t) + Du(t) + Y_C,\end{aligned} \quad (7)$$

where the constant vector Y_C is defined as

$$Y_C = Y_0 - (CX_0 + DU_0) \quad \text{with} \quad X_0 = -A^{-1}BU_0. \quad (8)$$

The application of the superposition principle shows that feeding (7) with the total input $u(t) = \tilde{u}(t) + U_0$, including also the constant bias component, leads to an output including both bias and small-signal components $\eta(t) \approx \tilde{\eta}(t) + Y_0$, where Y_0 is exact and $\tilde{\eta}(t)$ is approximated following the data-driven model order reduction process used to obtain $H(s) \approx \tilde{H}(s)$. Coherently, the initial condition X_0 of (7) is determined by the bias component U_0 according to (8), in agreement with the typical settings of any SPICE engine. Note that the states $x(t)$ and the associated operating point X_0 have no direct physical meaning, since they are associated to the black-box behavioral model resulting from the rational approximation.

B. Parameterized Affine Linearized Models

The affine linearized model (7) can be safely used to replace the original circuit block (1), as far as all signals remain in proximity of the reference operating point embedded in the model equations. However, from a system level perspective, the operating condition of the circuit is not known a priori, but results from the interaction of all the external circuits and terminations that are connected to its interface ports. Changing the loading conditions may lead to a modification of the operating point, making a given predetermined affine linearized model inadequate.

In order to guarantee that the model is instantiated according to the proper operating point, the affine linearized dynamics (7) can be generalized in such a way that the explicit dependence of the equations on the operating point is embedded in the model structure [14], [19]. Consider the *bias space* defining the set of all the possible bias configurations under which the circuit can operate

$$\mathcal{U}_0 = [\underline{U}_0^1, \overline{U}_0^1] \times [\underline{U}_0^2, \overline{U}_0^2] \times \cdots \times [\underline{U}_0^P, \overline{U}_0^P] \quad (9)$$

where U_0^i is the DC component of the circuit input at the i-th electrical port. It is assumed that for each bias condition $U_0 \in \mathcal{U}_0$, there exists a unique equilibrium point $\Xi_0 = \Xi_0(U)$ fulfilling (3). Omitting for brevity Ξ_0 in matrices (5), transfer functions (4) can be parameterized by $U_0 \in \mathcal{U}_0$ as follows

$$\tilde{H}(s, U_0) = \tilde{D}(U_0) + \tilde{C}(U_0)(sI_N - \tilde{A}(U_0))^{-1}\tilde{B}(U_0). \quad (10)$$

A reduced order model which incorporates in closed form the dependence of the small signal transfer function on the bias condition can be obtained starting from samples of (10), computed at discrete frequency-bias configurations

$$\tilde{H}_{k,m} = H(j\omega_k, U_{0m}), \quad k = 1, \dots K, \quad m = 1, \dots, M \quad (11)$$

which are again made available by a multivariate parametric AC sweep of the original circuit. Starting from the dataset (11), a parameterized small-signal model can be derived through various strategies, e.g, [20], [21] and the latest [22]. Here, we consider the so-called Parameterized Sanathanan-Koerner [15] (PSK) modeling framework, which provides a low order rational approximation based on the following model structure

$$H(s, U_0) = \frac{N(s, U_0)}{D(s, U_0)} = \frac{\sum_{i=0}^{n} \sum_{\ell=1}^{\bar{\ell}} R_{i,\ell}\, \zeta_\ell(U_0)\, \varphi_i(s)}{\sum_{i=0}^{n} \sum_{\ell=1}^{\bar{\ell}} r_{i,\ell}\, \zeta_\ell(U_0)\, \varphi_i(s)}. \quad (12)$$

The rational form of (12) is induced by the partial fraction basis $\varphi_0(s) = 1$, $\varphi_i(s) = (s - q_i)^{-1}$ where q_i are given (real) stable poles as in standard VF (complex-conjugate pairs can be used with simple modifications [18]). The multivariate basis functions $\zeta_\ell : \mathcal{U}_0 \to \mathbb{R}$, are responsible for representing the variations of the poles and the zeros of the transfer function, induced by the operating point parameterization. The unknown coefficients $R_{i,\ell} \in \mathbb{R}^{P \times P}$, $r_{i,\ell} \in \mathbb{R}$ are obtained using the PSK iteration, as introduced in [23]. The algorithm minimizes the model-vs-data error by iteratively solving a series of weighted least squares problems. This algorithm generalizes the standard Sanathanan-Koerner iteration [24] and the VF iteration to the parameterized case and is well-established. Details are therefore omitted here, we refer the reader to [15].

C. State-Space and Descriptor Realizations

A state space representation for the model structure (12) can be derived along the lines of [15]. We only report here the main results, since they are required for successive derivations.

Consider the three state space realizations of numerator, denominator, and augmented denominator of (12)

$$N(s, U_0) \leftrightarrow \Sigma_N = \left(\begin{array}{c|c} A_N & B_N \\ \hline C_N(U_0) & D_N(U_0) \end{array}\right) \quad (13)$$

$$D(s, U_0) \leftrightarrow \Sigma_1 = \left(\begin{array}{c|c} A_1 & B_1 \\ \hline C_1(U_0) & D_1(U_0) \end{array}\right) \quad (14)$$

$$D(s, U_0)I_P \leftrightarrow \Sigma_D = \left(\begin{array}{c|c} A_D & B_D \\ \hline C_D(U_0) & D_D(U_0) \end{array}\right), \quad (15)$$

where

$$\begin{aligned} A_D &= I_P \otimes A_1, & B_D &= I_P \otimes B_1, \\ C_D &= I_P \otimes C_1, & D_D &= I_P \otimes D_1 \end{aligned} \quad (16)$$

and $\otimes$ is the matrix Kronecker product. It can be shown that the small signal transfer function (12) admits the following

state space representation (we omit the parametric dependence on U_0 in the right-hand side for the sake of brevity)

$$\mathsf{H}(s, U_0) \leftrightarrow \left(\begin{array}{c|c} A_\mathsf{D} - B_\mathsf{D} D_\mathsf{D}^{-1} C_\mathsf{D} & -B_\mathsf{D} D_\mathsf{D}^{-1} \\ \hline C_\mathsf{N} - D_\mathsf{N} D_\mathsf{D}^{-1} C_\mathsf{D} & D_\mathsf{N} D_\mathsf{D}^{-1} \end{array} \right) \quad (17)$$

and the following equivalent descriptor realization

$$\underbrace{\begin{bmatrix} I_{n \times P} & 0 \\ 0 & 0 \end{bmatrix}}_{E} \begin{bmatrix} \dot{x} \\ \dot{w} \end{bmatrix} = \underbrace{\begin{bmatrix} A_\mathsf{D} & B_\mathsf{D} \\ C_\mathsf{D}(U_0) & D_\mathsf{D}(U_0) \end{bmatrix}}_{\mathcal{A}(U_0)} \begin{bmatrix} x \\ w \end{bmatrix} + \underbrace{\begin{bmatrix} 0 \\ -I_P \end{bmatrix}}_{\mathcal{B}} \tilde{u}$$

$$\tilde{y} = \underbrace{\begin{bmatrix} C_\mathsf{N}(U_0) & D_\mathsf{N}(U_0) \end{bmatrix}}_{\mathcal{C}(U_0)} \begin{bmatrix} x \\ w \end{bmatrix} \quad (18)$$

provided that $A_\mathsf{N} = A_\mathsf{D}$ and $B_\mathsf{N} = B_\mathsf{D}$. These conditions are easily enforced since the basis poles q_i defining $\varphi_i(s)$ are in common to numerator and denominator, so that the following diagonal realization ($q_i \in \mathbb{R}$) can be adopted

$$A_1 = \mathrm{diag}([q_1, q_2, \ldots, q_n]) \qquad \in \mathbb{R}^{n \times n} \quad (19)$$

$$B_1 = \begin{bmatrix} 1, 1, \ldots, 1 \end{bmatrix}^\top \qquad \in \mathbb{R}^{n \times 1} \quad (20)$$

$$C_1(U_0) = \sum_{\ell=1}^{\bar{\ell}} \zeta_\ell(U_0) \cdot C_{1,\ell} \qquad \in \mathbb{R}^{1 \times n} \quad (21)$$

$$D_1(U_0) = \sum_{\ell=1}^{\bar{\ell}} \zeta_\ell(U_0) \cdot d_{1,\ell} \qquad \in \mathbb{R}^{1 \times 1} \quad (22)$$

with

$$C_{1,\ell} = \begin{bmatrix} r_{1,\ell}, r_{2,\ell}, \ldots, r_{n,\ell} \end{bmatrix} \quad (23)$$

$$d_{1,\ell} = r_{0,\ell}, \quad (24)$$

and similarly for $C_\mathsf{N}(U_0)$, $D_\mathsf{N}(U_0)$. See [15] for details on handling complex basis poles. We remark that the equivalence of (18) with (17) holds whenever $D_1(U_0) \neq 0$ for all $U_0 \in \mathcal{U}_0$, a condition that is guaranteed by the proposed stability conditions, see Sec. IV. As a consequence, the descriptor system (18) is well-posed, regular, and impulse-free.

Once the small-signal model is available in form of (17) or (18), it can be augmented with the affine output term, which guarantees that the model provides the proper DC output for each possible bias condition included in $\mathcal{U}_0$. This is done by interpolation of data samples of the required map $Y_C(U_0) : \mathcal{U}_0 \to \mathbb{R}^P$, as explained in [14], [19].

From now on we will consider (18) as a reference model representation for our developments. The adopted model structure is therefore

$$E \begin{bmatrix} \dot{x} \\ \dot{w} \end{bmatrix} = \mathcal{A}(U_0) \begin{bmatrix} x \\ w \end{bmatrix} + \mathcal{B} u$$

$$y = \mathcal{C}(U_0) \begin{bmatrix} x \\ w \end{bmatrix} + Y_C(U_0) \quad (25)$$

where $E, \mathcal{A}(U_0), \mathcal{B}$ and $\mathcal{C}(U_0)$ are defined according to (18).

Models like (25) have been exploited in the literature by assuming that the biasing input U_0 does not depend on time. For instance, [14] considers uncertain Linear Time Invariant (LTI) systems in which the proper parameter configuration is set at the beginning of a transient simulation and remains unchanged during runtime operation. In our previous work [12],

such models were studied from the energetic perspective, with the objective of characterizing local dissipativity and energy exchanges with the environment through bias and small signal components. In this work, we provide another extension by letting the bias condition to be time-dependent.

III. PROBLEM SETTING

The main objective of this work is to construct reduced order affine linearized models that are able to mimic the input-output behavior of system (1) under small-signal conditions, but characterized by a possibly time-varying operating point. This variation may be triggered by changes in the loading conditions induced by terminations, or by control signals specifically designed to tune the operating point based on suitable performance goals (e.g., power consumption).

We split the input signal into its time-varying bias and small-signal components by generalizing (2) as

$$u(t) = U_0(t) + \tilde{u}(t), \quad (26)$$

where

- $U_0(t)$ is a slowly varying signal which attains values within the bias space

$$U_0(t) \in \mathcal{U}_0 \quad \forall t, \quad (27)$$

henceforth denoted as *bias component*;
- $\tilde{u}(t)$ is a small-signal input with $\tilde{u}(0) = 0$.

Under these conditions, a fixed model (7) is not suitable for representing the dynamics of (1), since the variations of the bias component $U_0(t)$ may drive the nonlinear system to operate around different equilibrium points.

Our derivations are based on the following

Assumption 1: For each $t^* \geq 0$, the nonlinear equation

$$F(\xi, U_0(t^*)) = 0 \quad (28)$$

has a unique solution $\xi = \Xi_0(t^*)$, and a small constant $\delta_\xi > 0$ exists such that each solution of (1) corresponding to input (26), obeys the inequality

$$\|\xi(t^*) - \Xi_0(t^*)\|_2 \leq \delta_\xi. \quad (29)$$

Assumption 1 requires that the nonlinear system is fast enough to respond almost instantaneously to variations in the biasing input, so that the corresponding time-varying local equilibrium point tracks continuously the variations of the input bias component. This assumption can be satisfied by limiting the spectrum of $U_0(t)$ to sufficiently low frequencies. The implications of this restriction will be documented on a practical example presented Section VI. If Assumption 1 holds, for every time instant the system trajectory $(\xi(t), u(t))$ is confined to a neighborhood of the particular state-input configuration $(\Xi_0(t), U_0(t))$ which satisfies

$$\begin{aligned} 0 &= F(\Xi_0(t), U_0(t)), \\ Y_0(t) &= G(\Xi_0(t), U_0(t)). \end{aligned} \quad (30)$$

Assuming that δ_ξ is small enough and (30) holds, the small-signal dynamics of (1) can be approximated by the time-varying linearization

$$\dot{\tilde{\xi}}(t) \approx F'_\Xi(\Xi_0(t), U_0(t)) \cdot \tilde{\xi}(t) + F'_U(\Xi_0(t), U_0(t)) \cdot \tilde{u}(t),$$
$$\tilde{\eta}(t) \approx G'_\Xi(\Xi_0(t), U_0(t)) \cdot \tilde{\xi}(t) + G'_U(\Xi_0(t), U_0(t)) \cdot \tilde{u}(t), \quad (31)$$

with $\tilde{\xi}(0) = 0$. In view of the one-to-one correspondence between $\Xi_0(t)$ and $U_0(t)$, (31) can be rewritten as

$$\dot{\tilde{\xi}}(t) \approx \tilde{A}(U_0(t)) \cdot \tilde{\xi}(t) + \tilde{B}(U_0(t)) \cdot \tilde{u}(t), \quad \tilde{\xi}(0) = 0$$
$$\tilde{\eta}(t) \approx \tilde{C}(U_0(t)) \cdot \tilde{\xi}(t) + \tilde{D}(U_0(t)) \cdot \tilde{u}(t). \quad (32)$$

Here $\tilde{A}, \tilde{B}, \tilde{C}, \tilde{D}$ are the matrices defined in (5). We notice that under Assumption 1, for each fixed time instant, the matrices entering (32) coincide with those entering (10), provided that $U_0(t) \in \mathcal{U}_0, \forall t$. Thus, we can easily generalize the parameterized modeling process of Sec. II-B to build a reduced order model representation for the desired map $U_0(t) + \tilde{u}(t) \to Y_0(t) + \tilde{\eta}(t)$. The process is as follows:

1) collect frequency samples (11) of the small-signal transfer function for fixed configurations of the bias condition;
2) build a parameterized transfer function of reduced order in the form of (12) by making use of the PSK algorithm;
3) cast the parameterized transfer function into the descriptor system (25) or into an equivalent netlist [2]. Up to this step, the procedure is the same as for standard parameterized macromodeling flows.
4) during a transient simulation, extract the bias input component $U_0(t)$ from the total input $u(t)$ and use this time-varying bias to instantiate the model parameters in (25) by setting $U_0 = U_0(t)$ at each time step.

The result of the procedure is a Linear-Parameter-Varying (LPV) affine model

$$E \begin{bmatrix} \dot{x} \\ \dot{w} \end{bmatrix} = \mathcal{A}(U_0(t)) \begin{bmatrix} x \\ w \end{bmatrix} + \mathcal{B} u$$
$$y = \mathcal{C}(U_0(t)) \begin{bmatrix} x \\ w \end{bmatrix} + Y_C(U_0(t)) \quad (33)$$

which is a generalization of (25) to the time-varying case. This model can seamlessly replace the original circuit block in a transient analysis. Due to the adopted data-driven order reduction process leading to a compact size of the state-space matrices in (33), significant speedup in runtime is expected.

In order to safely exploit model (33) in system-level simulations, two main problems need to be addressed and solved.

- if the dynamics of the original system (1) are known to be stable under inputs of type (26), this property must be inherited by the time-varying reduced order model. In fact, even if the "frozen-time" model (25) is uniformly stable for *constant* values of U_0 in the bias space, it is not guaranteed in general that the model will remain stable when a time variation $U_0(t)$ is induced and the system descriptor matrices become time-varying [25].
- during runtime operation, the bias component $U_0(t)$ must be estimated starting from the evolution of the full input $u(t)$, in order to provide a valid instantaneous parameterization of the time-varying model.

The main contributions of this work provide a solution to these two problems, discussed in Sec. IV and Sec. V, respectively.

IV. ENFORCING MODEL STABILITY

The stability characterization of multivariate rational models has been extensively considered in the literature, see e.g. [26], [15]. Most of the available results aim at constraining either model generation or model structure in order to guarantee the placement of the poles of $\mathsf{H}(s, U_0)$ in the open left-half complex plane for all the parameter configurations of interest. When employing model structure (12), this condition is fulfilled when the zeros of the denominator function $\mathsf{D}(s, U_0)$ have negative real part for each U_0. This can be guaranteed by constraining $\mathsf{D}(s, U_0)$ to be a positive real function over the entire frequency-parameter space, enforcing

$$\Re\{\mathsf{D}(\jmath\omega, U_0)\} > 0, \quad \forall \omega, \quad \forall U_0 \in \mathcal{U}_0, \quad (34)$$

in addition to technical conditions that are guaranteed by the adopted model structure. Both sampling-based [27] and sampling-free [28] methods have been proposed in the literature to enforce (34). We highlight that condition (34) does not force the overall transfer function $\mathsf{H}(s, U_0)$ to be positive real, but is only instrumental in enforcing the uniform stability of the model. Active circuits such as amplifiers are explicitly included in our formulation and are compatible with (34).

A. Preliminaries and Challenges

Frequency domain conditions like (34) can be used to test asymptotic stability of LTI systems, however, they do not guarantee stability of LPV equations (33). Therefore, some stronger conditions are required.

The characterization of the stability properties of LPV systems has been subject of intensive research in the fields of robust control and gain scheduling, see for instance [29], [30], [31], [32]. A standard approach is to embed in the modeling procedure the search for a Lyapunov function, which guarantees that the resulting descriptor system is *quadratically stable* (that is, exponentially stable and admits a quadratic Lyapunov function), as defined below in Theorem 1. This strong characterization entails the asymptotic stability of system (33) under any possible time domain evolution of the parameters $U_0(t)$. We refer to [33], for a complete theoretical framework.

The main key result on which we build our developments is the following [16, Theorem 2.4.4]

Theorem 1 (quadratic stability for descriptor systems): the descriptor LPV system

$$E \begin{bmatrix} \dot{x} \\ \dot{w} \end{bmatrix} = \mathcal{A}(U_0(t)) \begin{bmatrix} x \\ w \end{bmatrix} \quad (35)$$

is quadratically stable if there exists

$$Q(U_0) = \begin{bmatrix} Q_1 & 0 \\ Q_2(U_0) & Q_3(U_0) \end{bmatrix} \quad (36)$$

with $Q_1 \in \mathbb{R}^{(nP \times nP)}$, $Q_1 = Q_1^\top \succ 0$, $Q_2 : \mathcal{U}_0 \to \mathbb{R}^{P \times n}$ and $Q_3 : \mathcal{U}_0 \to \mathbb{R}^{P \times P}$ such that the inequality holds

$$\mathcal{A}(U_0)^\top Q(U_0) + Q(U_0)^\top \mathcal{A}(U_0) \prec 0 \quad \forall U_0 \in \mathcal{U}_0. \quad (37)$$

In principle, Theorem 1 provides sufficient conditions that (33) must fulfill in order to be quadratically stable. However, such conditions cannot be enforced during the model generation, for two main reasons:

1) The entries of the state matrix $\mathcal{A}(U_0)$ are determined by the unknown model coefficients, according to (21) and (22). Considering these coefficients and $Q(U_0)$ as unknown variables, (37) becomes a *non-convex* bilinear matrix inequality (BMI) and thus cannot be solved efficiently as the number of unknowns becomes large.

2) Condition (37) is required to hold uniformly over the whole parameter space $\mathcal{U}_0$, imposing an infinite set of constraints.

These considerations would translate in the necessity to perform the model estimation under an infinite number of BMI constraints, in order to guarantee the quadratic stability of (33). This scenario is obviously impractical.

B. Proposed framework for quadratic stability enforcement

Our main approach to guarantee the quadratic stability of the proposed LPV model is to derive a sufficient condition by suitably constraining the model structure and its coefficients. We see below that adopting basis functions ζ_ℓ that are positive and forming a partition of unity, leads to quadratic stability conditions that can be cast as a *finite* set of LMIs. Such constraints are convex and can be easily incorporated in the model generation algorithm, leading to a formulation based on semidefinite programs that can be efficiently handled by standard convex optimization solvers.

We now formulate and prove our main result.

Theorem 2 (Sufficient conditions for quadratic stability): Let the basis functions $\zeta_\ell(U_0)$ satisfy the conditions

$$\sum_{\ell=1}^{\bar{\ell}} \zeta_\ell(U_0) = 1 \quad \forall U_0 \in \mathcal{U}_0 \tag{38}$$

$$\zeta_\ell(U_0) \geq 0 \quad \forall U_0 \in \mathcal{U}_0, \quad \ell = 1, \ldots, \bar{\ell}. \tag{39}$$

Then, the LPV system (33) is quadratically stable if there exists $Q_1^* \in \mathbb{R}^{n \times n}$ such that $Q_1^* = Q_1^{*\top} \succ 0$ and

$$\begin{bmatrix} A_1^\top Q_1^* + Q_1^* A_1 & Q_1^* B_1 - C_{1,\ell}^\top \\ B_1^\top Q_1^* - C_{1,\ell} & -2d_{1,\ell} \end{bmatrix} \prec 0 \quad \ell = 1, \ldots, \bar{\ell}. \tag{40}$$

Proof: Consider first the descriptor state matrix associated to (33) for the single-input-single-output case, $P = 1$

$$\mathcal{A}(U_0) = \begin{bmatrix} A_1 & B_1 \\ C_1(U_0) & D_1(U_0) \end{bmatrix}. \tag{41}$$

Applying Theorem 1 to the matrix $\mathcal{A}$ from (41) and

$$Q = \begin{bmatrix} Q_1^* & 0 \\ 0 & -1 \end{bmatrix}$$

one proves that (41) is quadratically stable if $Q_1^* = Q_1^{*\top} \succ 0$ obeys the inequalities

$$\begin{bmatrix} A_1^\top Q_1^* + Q_1^* A_1 & Q_1^* B_1 - C_1(U_0)^\top \\ B_1^\top Q_1^* - C_1(U_0) & -2D_1(U_0) \end{bmatrix} \prec 0 \quad \forall U_0 \in \mathcal{U}_0. \tag{42}$$

Substituting (21) and (22) into (42) leads to the equivalent condition

$$\begin{bmatrix} A_1^\top Q_1^* + Q_1^* A_1 & Q_1^* B_1 - \sum_{\ell=1}^{\bar{\ell}} \zeta_\ell(U_0) \cdot C_{1,\ell}^\top \\ B_1^\top Q_1^* - \sum_{\ell=1}^{\bar{\ell}} \zeta_\ell(U_0) \cdot C_{1,\ell} & -\sum_{\ell=1}^{\bar{\ell}} \zeta_\ell(U_0) \cdot d_{1,\ell} \end{bmatrix} \prec 0 \tag{43}$$

that must hold $\forall U_0 \in \mathcal{U}_0$. In view of (38), one has

$$A_1 = A_1 \sum_{\ell=1}^{\bar{\ell}} \zeta_\ell(U_0), \quad B_1 = B_1 \sum_{\ell=1}^{\bar{\ell}} \zeta_\ell(U_0) \tag{44}$$

so that (43) shapes into

$$\sum_{\ell=1}^{\bar{\ell}} \zeta_\ell(U_0) \begin{bmatrix} A_1^\top Q_1^* + Q_1^* A_1 & Q_1^* B_1 - C_{1,\ell}^\top \\ B_1^\top Q_1^* - C_{1,\ell} & -2d_{1,\ell} \end{bmatrix} \prec 0, \ \forall U_0 \in \mathcal{U}_0 \tag{45}$$

Due to (39), condition (45) is entailed by the discrete set of LMIs (40). This proves the result for the case $P = 1$.

The general case $P > 1$ is proved by applying Theorem 1 to the matrix $\mathcal{A}(U_0)$ whose blocks are defined in (16)

$$\mathcal{A}(U_0) = \begin{bmatrix} I_P \otimes A_1 & I_P \otimes B_1 \\ I_P \otimes C_1(U_0) & I_P \otimes D_1(U_0) \end{bmatrix}, \tag{46}$$

and the matrix

$$Q = \begin{bmatrix} I_P \otimes Q_1^* & 0 \\ 0 & -I_P \end{bmatrix},$$

where $Q_1^* = Q_1^{*\top} \succ 0$ is a matrix that satisfies (42). Condition (37) shapes into

$$\mathcal{S} \prec 0 \quad \forall U_0 \in \mathcal{U}_0, \tag{47}$$

with

$$\mathcal{S} = \begin{bmatrix} I_P \otimes (A_1^\top Q_1^* + Q_1^* A_1) & I_P \otimes (Q_1^* B_1 - C_1(U_0)^\top) \\ I_P \otimes (B_1^\top Q_1^* - C_1(U_0)) & -I_P \otimes (2D_1(U_0)) \end{bmatrix}$$

A similarity transformation $\bar{\mathcal{S}} = T^\top \mathcal{S} T$, where T is an appropriate permutation matrix, leads to

$$\bar{\mathcal{S}} = I_P \otimes \begin{bmatrix} A_1^\top Q_1^* + Q_1^* A_1 & Q_1^* B_1 - C_1(U_0)^\top \\ B_1^\top Q_1^* - C_1(U_0) & -2D_1(U_0) \end{bmatrix} \tag{48}$$

which is a block-diagonal repetition of (42), being thus negative definite, along with $\mathcal{S}$, whenever Q_1^* satisfies (40). This completes the proof. ∎

C. Discussion

Theorem 2 provides sufficient conditions for the quadratic stability of the proposed affine LPV system (33), which can be enforced during the model generation very easily. In fact, conditions (40) constitute a finite set of small-size LMIs, where the free variables are $Q_1^* \in \mathbb{R}^{n \times n}$, $C_{1,\ell} \in \mathbb{R}^{1 \times n}$, and $d_\ell \in \mathbb{R}$ for $\ell = 1, ..., \bar{\ell}$. Note that the latter include only the unknown coefficients defining the (scalar) denominator in (12), since the PSK iteration is usually cast as an iterative least squares problem that eliminates the numerator unknowns in a preprocessing step, see [34]. Overall these quadratic stability conditions amount to $\bar{\ell}$ independent LMI constraints, each of

size $(n+1)\times(n+1)$ on a total of $n(n+1)/2+(n+1)\bar{\ell}$ degrees of freedom. These constraints are to be combined with the least squares problem on the $(n+1)\bar{\ell}$ denominator coefficients.

Some remarks are in order.

Remark 1: In order to remove the bilinear dependence of (37) on the unknowns and derive the proposed linearized quadratic stability constraints, we have simplified the structure of the Lyapunov function $Q(U_0)$ that enters in the general Theorem 1. In particular, for constant values of the involved matrices, setting $Q_3(U_0) \equiv -1$ has no real influence on the results, except for an indirect renormalization of all coefficients of the model. Instead, imposing $Q_2(U_0) \equiv 0$ may introduce some degree of conservatism, and could lead to potential losses of model accuracy by over-constraining the model coefficients, which in turn constrain the set of the allowed parameterized poles trajectories. We however have observed no significant loss of accuracy by imposing the proposed constraints in place of state of the art uniform stability constraints valid for frozen parameter macromodels (e.g. by means of the strategy advised in [27]). See Sec. VI.

Remark 2: The proposed framework imposes a restriction on the choice of parameter-dependent basis functions $\zeta_\ell(U_0)$, which must be non-negative and represent a partition of unity over the entire bias space. In this work, we adopt the multivariate Bernstein polynomials [35], which are compliant with these constraints. In the univariate case, Bernstein polynomials $b_{\nu,\bar{\nu}}(\theta)$ of the degree $\bar{\nu}$ in the normalized domain $\theta \in [0,1]$ are

$$b_{\nu,\bar{\nu}}(\theta) = \binom{\bar{\nu}}{\nu}\theta^\nu(1-\theta)^{\bar{\nu}-\nu}, \quad \nu = 0,\ldots,\bar{\nu}. \tag{49}$$

For higher dimension $P > 1$, the multivariate basis functions ζ_ℓ are constructed as Cartesian products of univariate Bernstein polynomials as follows

$$\zeta_\ell(U_0) = \prod_{i=1}^{P} \zeta_{\ell_i}(U_0^i), \ \zeta_{\ell_i}(U_0^i) = b_{\ell_i,\bar{\ell}_i}(\theta^i), \ \theta_i = \frac{U_0^i - \underline{U}_0^i}{\overline{U}_0^i - \underline{U}_0^i}.$$

Here $0 \leq \ell_i \leq \bar{\ell}_i$ is the index corresponding to the i-th coordinate in the bias space, and all possible P-tuples of indices $(\ell_1,\ldots,\ell_P)$ are indexed by $\ell = 1,\ldots,\bar{\ell} = \prod_i(1+\bar{\ell}_i)$.

Remark 3: Our derivations are based on the assumption that for any set of biasing inputs $U_0 \in \mathcal{U}_0$, the nonlinear system (1) operates around a stable working point defined by equations (3). This property is inherited by the parameterized macromodel whenever constraints (40) are used for its generation. However, it is well known that when active circuit blocks are interconnected with (even passive) termination networks, the overall behavior of the whole system is not guaranteed to be stable. It is thus of interest to ask whether a given reference nonlinear circuit and the corresponding affine linearized equivalent (7) are both stable (or unstable) under the same loading conditions.

This is not true in general, due to the unavoidable differences between the local behavior of the reference circuit and that of the macromodel: these differences are introduced both by the linearization process and by the rational approximation used to build the reduced order model. Nevertheless, provided
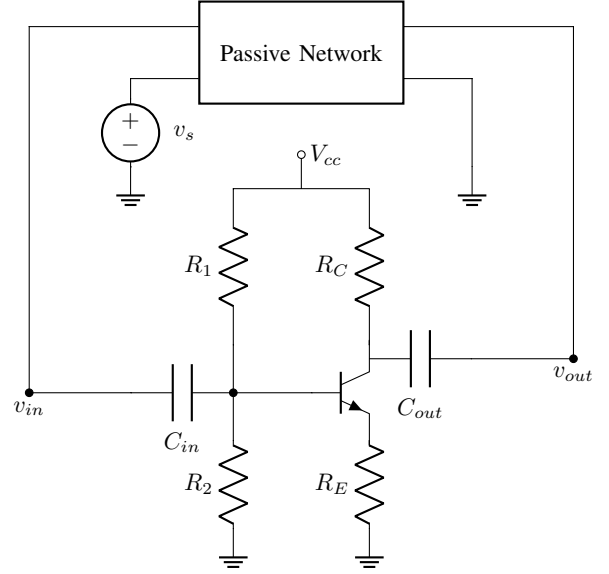

Fig. 1. A common emitter amplifier ($C_{in} = C_{out} = 10 \ \mu$F, $R_1 = 4 \ k\Omega$, $R_2 = 1 \ k\Omega$, $R_C = 110 \ \Omega$, $R_E = 20 \ \Omega$ and $V_{cc} = 10 \ $V) interconnected with a passive two-port network (see text).

that the linearization error is negligible, and that the small-signal approximation $\mathsf{H}(s,U_0) \approx \tilde{\mathsf{H}}(s,U_0)$ holds with high accuracy, then it may be argued that a given termination that destabilizes the macromodel will also destabilize the original circuit, and vice versa. Note that, in this situation, the unstable behavior of both circuits would drive the signals outside the small-signal regime, making the proposed macromodel invalid.

As an illustrative example, consider the simple common emitter amplifier circuit depicted in Fig.1, for which a linearized macromodel was derived around its stable operating point. The small-signal transfer function has a maximum gain about 5.2. We then applied the procedure of [36, Sec. 4.1] to find a passive two-port network that, when interconnected to the macromodel, leads to an unstable system, in this case with a pair of complex conjugate poles with positive real part $p_{1,2} = +166 \pm j628 \ $rad/s. Using this termination, we performed a transient analysis of both macromodel and reference nonlinear circuit using a sinusoidal excitation $v_s(t)$ with amplitude 1 μV and frequency 100 Hz. The resulting output voltages are depicted in Fig. 2. Both reference and macromodel circuits are indeed unstable, with agreement only up to a finite time horizon (about 80 ms). For later times, the reference circuit undergoes saturation, making the small-signal linearization invalid.

D. Uniform and quadratic stability of parameterized macromodels

The proposed set of linearized quadratic stability constraints (40) can be seen as more general (yet restrictive) conditions for ensuring the uniform stability of standard LTI parameterized macromodels, where the parameters are constant. These are obviously a particular case of LPV systems, where time variation of the parameters is suppressed. Therefore, conditions (40) provide a novel and efficient framework
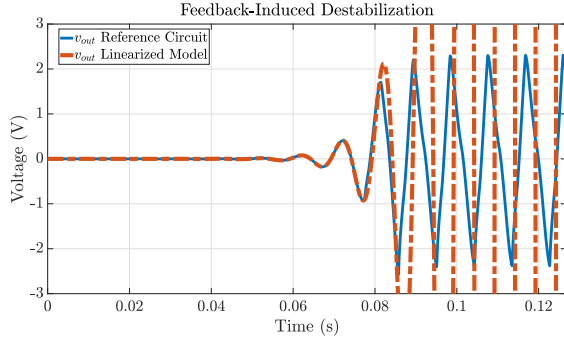
Fig. 2. Transient analysis of the unstable electrical network depicted in Fig. 1. Reference nonlinear circuit and linearized model are in agreement up to a given time horizon, after which the small-signal assumption does not hold.
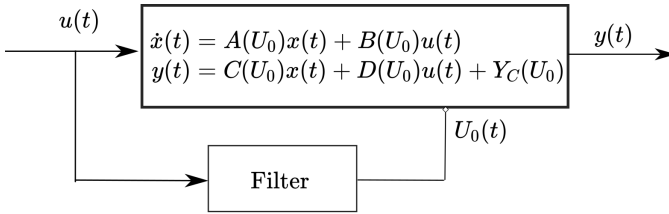

Fig. 3. The proposed model structure augmented with a low-pass filter aimed at extracting the low frequency content of the bias component and provide the instantaneous parameterization to the linearized dynamics.

for constraining uniform stability of multivariate macromodels, as an alternative to the consolidated condition (34).

It is interesting to note that both (34) and proposed conditions (40) provide a certification of model stability based on energetic properties of the model denominator function $D(s, U_0)$. In short, if $D(s, U_0)$ represents a passive system, then its inverse is also passive and both zeros and poles have a negative real part [27]. Condition (34) implies passivity based on a frequency-domain positive realness condition. Conversely, the proposed LMI conditions (40) provide a characterization of denominator passivity through the well known Kalman-Popov-Yakubovich (KYP) lemma [37], here restated for the parameterized case as

$$\forall U_0 \in \mathcal{U}_0, \; \exists \, Q(U_0) = Q(U_0)^\top \succ 0 \quad \text{such that}$$
$$\begin{bmatrix} A_1^\top Q(U_0) + Q(U_0)A_1 & Q(U_0)B_1 - C_1(U_0)^\top \\ B_1^\top Q(U_0) - C_1(U_0) & -2D_1(U_0) \end{bmatrix} \prec 0 \quad (50)$$

with the additional assumption that $Q(U_0) = Q_1$. In other words, the adopted formulation is equivalent to a stronger version of the KYP condition (50) with a constant storage function.

V. EXTRACTION OF TIME-VARYING BIAS COMPONENTS

The practical exploitation of model structure (33) for time domain simulations requires the availability of the instantaneous input bias component $U_0(t)$, to be provided as a parameter for the descriptor matrices (33). However, during a transient analysis, the signal decomposition (26) is not defined uniquely, as the only available numerical quantity is the full input signal $u(t)$ at the circuit interface. Therefore, the exploitation of (26) is practically applicable only in view

of an automated procedure aimed at isolating the bias and the small signal components.

Considering Assumption 1 (that requires U_0 to vary sufficiently slowly), we suppose that the spectrum of $U_0(t)$ is confined to a sufficiently narrow low-frequency band, to guarantee the validity of the proposed time-varying linearization. It is thus intuitive that the required parameterization can be obtained from the input signal by means of a low-pass filtering operation. Hence, we propose the augmented model structure shown in Fig. 3, which embeds a low-pass filter aimed at extracting the value of the instantaneous bias component from the whole model input.

The design of such a filter must be compliant with the requirements of our main assumption; in particular, it must provide a parameterization such that (29) holds with sufficiently small δ_ξ. However, since the non-linear equations (1) are not available in closed form, no analytical methods based on the native circuit description can be exploited to derive an exact characterization of the frequency domain properties that $U_0(t)$ must fulfill, in order to maintain the validity of the proposed approximation. Due to this limitation, only heuristic criteria based on experimental (simulated) data regarding the circuit under modeling can be employed to design the filter. We propose the following procedure:

1) Build the low-order small-signal transfer function (12).
2) Sample the poles of the transfer function over the bias space $\mathcal{U}_0$. This operation is not computationally expensive since the order n of the model is low.
3) Determine the angular frequency ω_p of the slowest pole of the parameterized transfer function.
4) Set the cut-off frequency of the filter $\omega_c = \rho \, \omega_p$, with $\rho \le 0.1$
5) Build a second order Butterworth filter of unit gain and cut-off frequency ω_c.

The above procedure is aimed at guaranteeing a sufficiently slow variation of the bias parameter, in compliance with previous results concerning LPV models derived from frozen-parameter configurations of the underlying system, see e.g. [38], [39], [40]. Whenever an a-priori knowledge of the frequency content of the bias input $U_0(t)$ is available, it can be used to tune the value of the ratio ρ.

In principle, time-domain data could also be exploited in the design of the desired filter, based for example on the maximization of the accuracy of the model against reference time domain training samples. In our framework, retrieving time domain data from the original circuit description is extremely expensive in terms of time requirements, as will be shown in the experimental section. Additionally, due to the non-linear nature of equations (1), time-domain approaches would not provide additional warranties of accuracy when the model is subject to input profiles that are different from those used to guide filter design. Time-domain approaches are thus impractical and beyond the scope of this work.

A. Alternative time-varying parameterizations

Up to now, our discussion has been focused on the generation of linearized models in which the variation of the

operating point is induced by slowly varying components of the electrical quantities imposed at the circuit block interfaces.

Model structure (33) can be exploited also to simulate variations of the circuit working condition as induced by external environmental parameters on which (1) may depend, such as temperature. The simplest scenario is the application of a known instantaneous profile, such e.g. representing a temperature profile induced by heating. A more complex scenario is a coupled electro-thermal or even multiphysics simulation, where the parameters are obtained as a result of a co-simulation of an associated thermal or multiphysics model.

In both the above-mentioned scenarios, it is assumed that the actual parameter value is available in some form as a variable that is independent on the electrical port signals. Therefore there is no need to make use of any filtering operation to derive the instantaneous working condition. In next section, we show an example of the first scenario, where a given temperature profile is applied at runtime. Coupled multiphysics simulations are left as a future investigation.

VI. NUMERICAL EXPERIMENTS

A. A Low Dropout Regulator Schematic

The first example provides a proof-of-concept validation of the proposed modeling framework. As reference circuit, we consider the CMOS Low Dropout (LDO) regulator design first proposed in [41]. The circuit schematic was instantiated in the LTSpice environment, without taking into account any additional layout description or packaging parasitics. This regulator provides a nominal output voltage $V_L = 2.8$ V for load currents values $I_L \in [0, 50]$ mA, with a minimum recommended DC input voltage $V_{DD} = 2.9$ V.

We modeled the circuit through its 2-port Hybrid representation, considering as port variables the input voltage (port 1) and the load current (port 2). For this test case, we fixed a reference load current $U_0^2 \equiv I_L = 10$ mA, while allowing the input voltage to vary within the set $U_0^1(t) \equiv V_{DD}(t) \in [2.85, 3]$ V, in order to stress the non-linear degradation of the power supply rejection at low input voltages. The considered bias space is therefore the set $\mathcal{U}_0 = [2.85, 3]$ V $\times$ 10 mA.

We sampled the bias space by collecting $M = 20$ distinct small-signal frequency responses at different DC levels of the input voltage, and we built a reduced order model of order $n = 8$ by applying the quadratic stability constraints (40). The poles and the zeros of the model were both parameterized by means of third order Bernstein polynomials. The frequency-domain fitting required 6.2 s. Figure 4 reports the results for two elements of the matrix transfer function, confirming the excellent accuracy of the model against the reference data. A low-pass filter with $\rho = 0.05$ and a cut-off frequency $\omega_c = 2\pi 800$ rad/s completes the model structure according to Fig. 3. The model was finally synthesized as a behavioral netlist, implemented in the LTSpice environment.

A set of transient analyses was performed in order to test the time domain performance of the proposed LPV behavioral

model against the reference transistor-level schematic. To this aim, we defined the following testing input signals

$$
\begin{aligned}
u^1(t) &= a_1 \sin(2\pi f_1 t) + \frac{b}{1 + e^{-k(t-0.09)}} + 2.85 \text{ V} \\
u^2(t) &= a_2 \sin(2\pi \sqrt{2} f_1 t) + I_L
\end{aligned}
\tag{51}
$$

where coefficients $a_1 = 5$ mV, $a_2 = 1$ mA and $f_1 = 10$ kHz define the small signal quantities. A variation of the operating point is induced by the second term in $u^1(t)$, with a slew rate parameterized by $b = 0.15$ V and by the shape factor k. A transient analysis was repeated for $k = 100, 200, \dots, 1000$, in order to assess the ability of the model to track increasingly faster operating point variations. The considered bias profiles are depicted in Fig. 5.

The regulated voltage returned by the model prediction was compared with the transistor-level reference for the ten considered test cases, by computing the RMS value of the corresponding deviation. The results are reported in the top panel of Fig 6, while the bottom panel reports the transient regulated voltage of model and true circuit for one case $k = 500$ (similar results were obtained for all values of k). We observe that the error remains quite small for all the considered bias profiles, although it increases slightly for faster bias variations. This behavior is expected, since faster variations are likely to be more difficult to track by the low-pass filter.

The necessity of a LPV model structure that embeds time-varying small-signal parameters is confirmed by Fig. 7. Here, the transient results obtained by a fixed model with LTI structure and constant state-space matrices defined by a prescribed operating point $U_0^1 = 2.85$ V are reported, by letting the input bias component switch according to (51) with $k = 500$. In this experiment, the evolution of the bias component is not tracked by the model. The results show that the LTI model is not able to reproduce the correct voltage regulation behavior of the original circuit as the input voltage drifts to a higher value. On the other hand, the proposed LPV model structure adaptively tracks the operating point variation and recovers both the trend and the small signal variations of the output voltage (bottom panel of Fig. 6).

B. A Post-Layout LDO Regulator Design

We now consider a more realistic application scenario for the proposed modeling framework, by taking into account a complete LDO voltage regulator circuit design, including its parasitics obtained from a post-layout extraction.

We instantiated in the Cadence environment the Only-MOS regulator design proposed in [42]. This design is characterized by low quiescent current and is designed for low-power applications, with a maximum nominal load current $I_L = 10$ mA and a minimum rated input voltage $V_{DD} = 0.9$ V. The circuit was designed according to the reference specifications, making use of a 40 nm CMOS process. The resulting layout takes a 0.0045 mm^2 area.

Similarly to the schematic of Sec. VI-A, the device was modeled as a 2-Port system in hybrid representation. For this test case, we fixed the bias level of the input voltage to
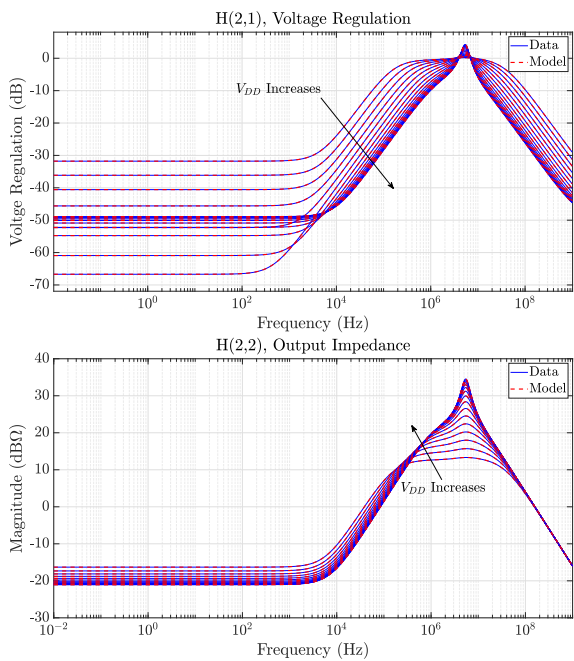
Fig. 4. Two elements of the transfer function for the LDO schematic test case. The parameterization is induced by the DC value of the input voltage. Both training and validation samples are shown.
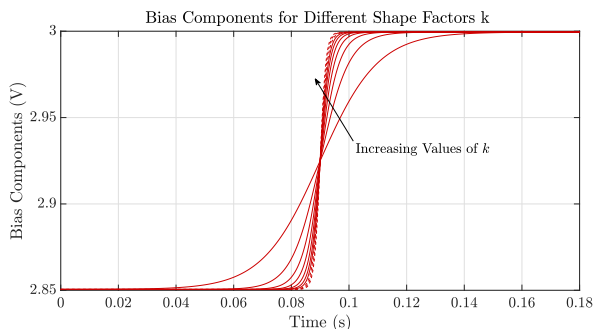

Fig. 5. Time variation of the the bias component $U_0^1(t)$ for the LDO schematic test case, for different values of $k = 100, 200, \ldots, 1000$.

$U_0^1 \equiv V_{DD} = 0.9$ V, while allowing load current to span the entire operating range, so that $U_0^2 \equiv I_L \in [0, 10]$ mA. We derived a model with $n = 9$ parameterized poles starting from $M = 50$ frequency responses obtained at different load current configurations, using a polynomial order $\bar{\ell} = 5$ for numerator and denominator. The model generation time was 8.6 s. The accuracy of the fitting is confirmed in Fig. 8, where no visible difference between the model and the reference small-signal responses can be noted, throughout the entire bias space. Finally, a low-pass filter with cut-off frequency $\omega_c = 2\pi 500$ rad/s was added to complete the LPV model structure (Fig. 3).

The resulting LPV model was used to simulate a transition from a low-power ($I_L = 0.5$ mA) to a higher consumption state $I_L = 2$ mA, with a transition time $\Delta t = 6$ ms. A time-varying noise signal with flat power spectrum limited to the band $1 - 10$ kHz and amplitude 0.2 mA was added to the output current, to represent a small-signal variation around
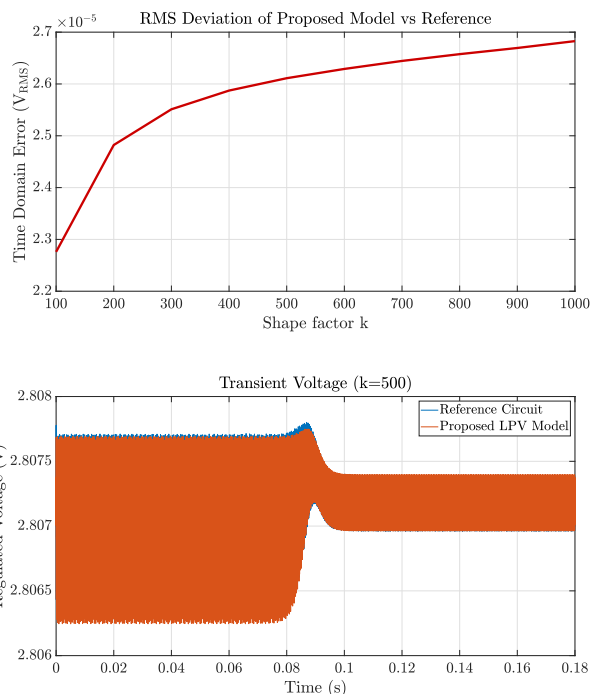

Fig. 6. LDO schematic test case. Top panel: RMS deviation of model wrt transistor-level response, as a function of the slew rate of input bias variation (see Fig. 5). Bottom panel: transient regulated voltages of model and transistor-level circuit for the case $k = 500$.
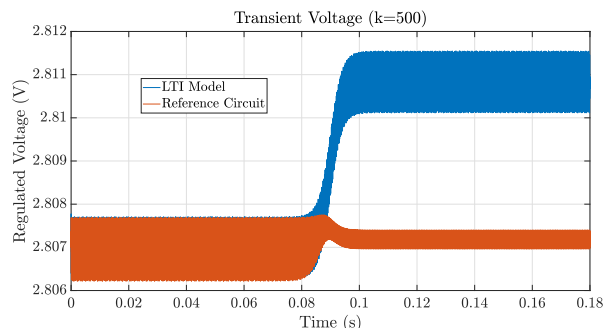

Fig. 7. LDO schematic test case: as in Fig. 6 (bottom panel), but using a fixed LTI model, with constant state-space matrices. This model cannot track the variation of the operating point as the input bias component switches to another DC level.

I_L. Similarly, a 20 mV small-signal variation with the same bandwidth was added to the input voltage.

The model was istantiated as an equivalent SPICE netlist in the LTSpice environment. The results of the simulation related to the regulated voltage are provided in Fig. 9, where we compare the model response against the reference device data. The results show that the model is accurate for the whole simulation length, and that the accuracy is preserved during the transition. The reference transistor-level simulation was performed using Cadence 6.1.7-64b + Spectre 18.1.0-64b enviroment into a HP Proliant DL580 Server featuring 72-parallel-CPU Intel Xeon Gold 6140M and 128GB RAM. The total run-time was approximately 13 minutes. The same transient analysis using the proposed model was performed in
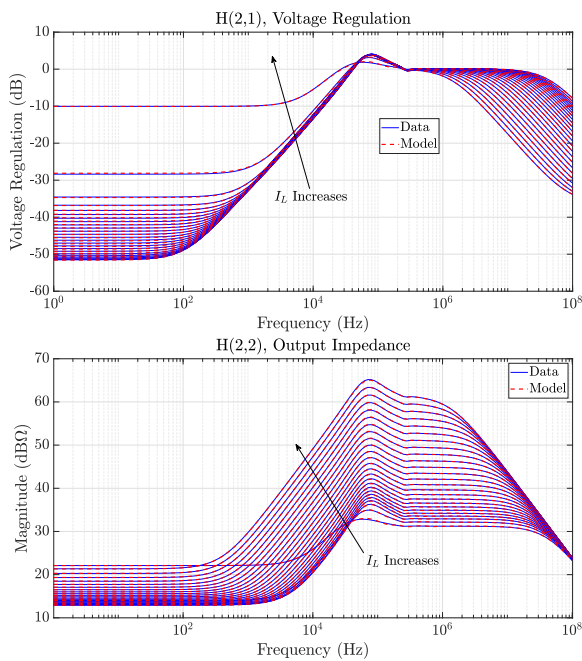
Fig. 8. Two frequency responses of the post-layout LDO test case. The parameterization is induced by the DC value of the load current in the range $[0, 10]$ mA. Only validation samples are shown.

LTSpice on a different machine, equipped with Intel Core i9 7900X CPU and 64 GB of RAM. The resulting runtime was 16 s, corresponding to a $50\times$ speed up.

To further validate the model, we simulated an additional operating point variation scenario, switching from a load current $I_L = 5$ mA to $I_L = 8$ mA in $\Delta t = 6$ ms, and using a small-signal component with amplitude 0.5 mA. The results are reported in Fig. 10. Also in this case the LPV model is in full agreement with the reference data, confirming the validity of the proposed approach.

C. Transient with given temperature profile

In this final experiment, we illustrate how the proposed LPV model structure can be adapted and exploited to track variations of environmental quantities during a transient analysis. We consider the LDO regulator already studied in Sec. VI-B, and we perform a transient analysis including a time variation of the device temperature. The LPV model was constructed by fixing the DC levels of the port variables to $V_{DD} = 1$ V and $I_L = 50$ μA, and by collecting a set of $M = 26$ parameterized small-signal transfer functions for a broad range of operating temperature conditions $T \in [-25, 100]$ °C. This data was used to generate a model with dynamic order $n = 8$ and third-order parameterization. The modeling procedure required 6.8 s. The resulting model accuracy is illustrated in Fig. 12. In addition, we have generated a model of the same order by enforcing the uniform stability constraints proposed in [27] for parameterized LTI macromodels, in place of (40); in Fig. 13 we compare the output impedance of the two models for different temperature values, showing that no visible degradation of the accuracy is induced when the constraints from [27] are replaced by our constraints (40).
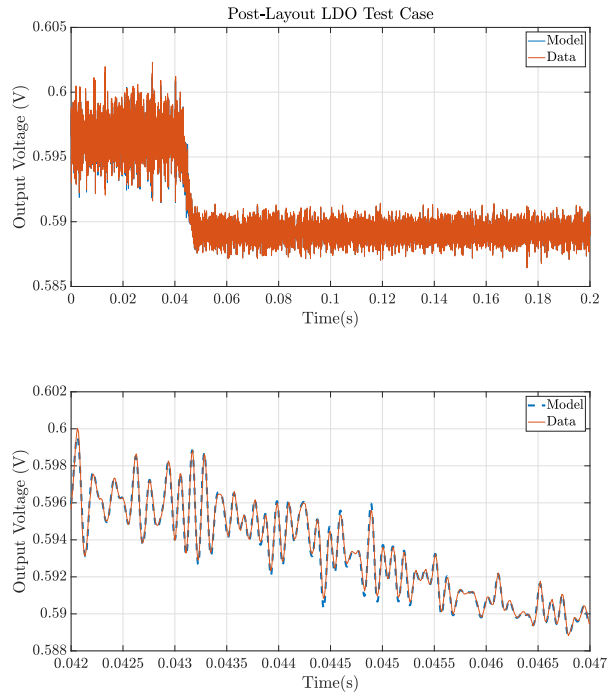

Fig. 9. Post-layout LDO test case. Top panel: regulated output voltage during an operating point transition from $I_L = 0.5$ mA to $I_L = 2$ mA; bottom panel: zoom on the transition time window.
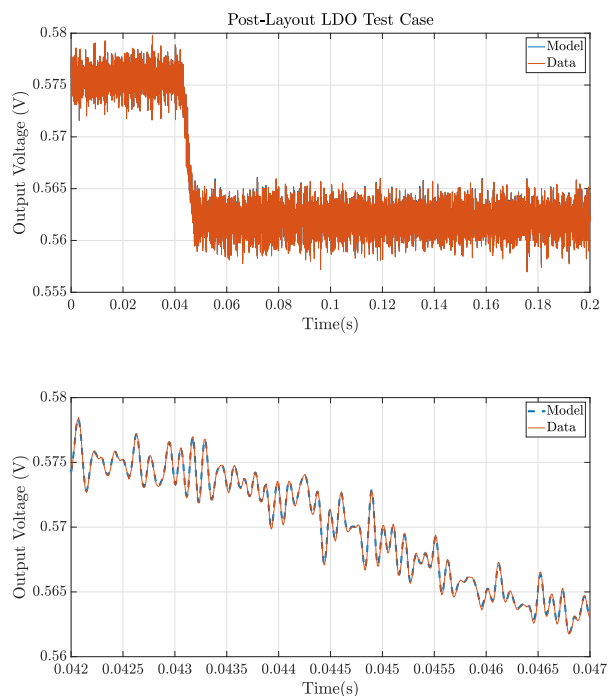

Fig. 10. Post-layout LDO test case. As in Fig. 9, but for an operating point transition from $I_L = 5$ mA to $I_L = 8$ mA.
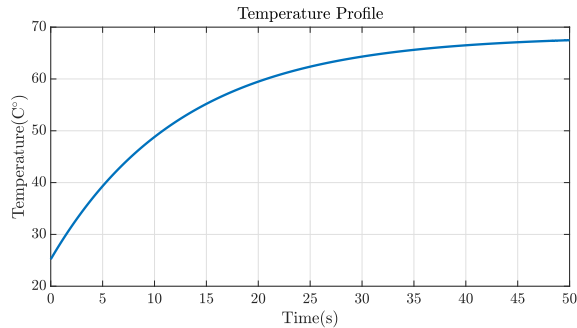
Fig. 11. The temperature profile used to perform the transient analysis of the LDO under time-varying environmental conditions.
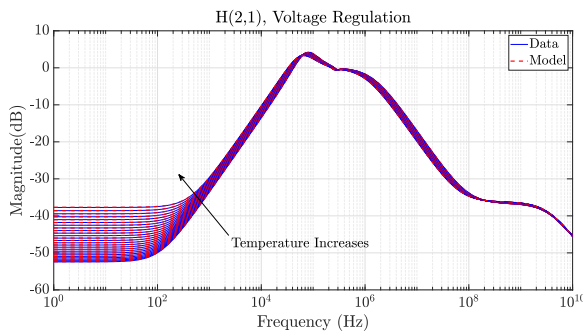

Fig. 12. Validation of the post-layout LDO model, parameterized by device temperature. The figure compares the model with the reference small-signal voltage regulation transfer function, for the temperature operating range $T \in [-25, 100]$ °C

For this illustrative example, the real-time temperature parameterization is injected directly into the model coefficients by making use of the temperature profile shown in Fig. 11, which simulates the variation induced by a CPU heating [43]. A band-limited small-signal component was added to the input voltage, with amplitude 30 mV and power spectrum limited to 100 Hz, with a peak around the line frequency at 50 Hz. A reference transient response was computed in the Cadence environment. Due to the extremely long duration of the transient, this simulation required approximately 24 hours to be performed.

The proposed model was instantiated and simulated with LTSpice in about 20 minutes, with a speed-up of about $100\times$. Figure 14 compares the transient evolution of the regulated voltage for both proposed model and transistor-level reference over three different time windows associated to different local temperature values. The figure reports also the results of a transient simulation performed with an ad hoc solver written in MATLAB and based on a simple backward Euler integration of the LPV model. Although this code is prototypal and non-optimized, the entire simulation required only 44 s, with further speedup with respect to a conventional SPICE implementation. Both reference and the two LPV model simulations provided compatible results, with no visible loss of accuracy.

VII. CONCLUSIONS

This work proposed a novel strategy for the generation of reduced-order Linear Parameter Varying (LPV) macromodels,
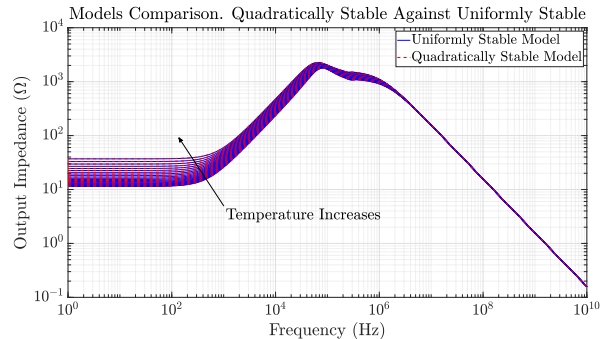

Fig. 13. Comparison between the output impedance of two models of the LDO circuit, obtained by enforcing the uniform stability constraints as in [27] and the proposed quadratic stability constraints (40) respectively.
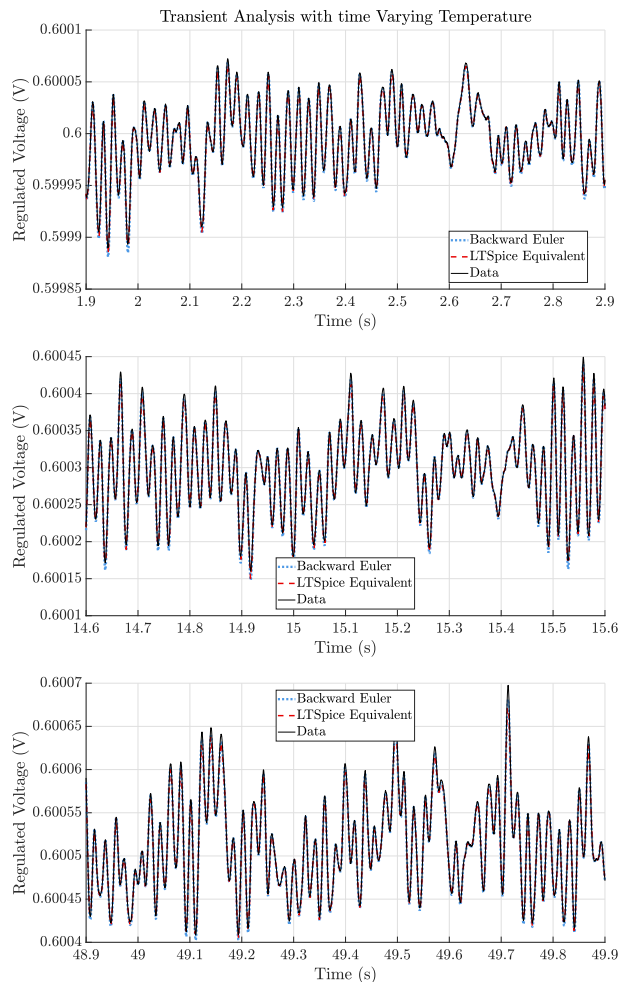

Fig. 14. Transient analysis of the post-layout LDO with time-varying temperature over three time windows extracted from the whole simulation, representative of different instantaneous temperature values. Top panel: $T \approx 32°$C. Middle panel: $T \approx 55°$C. Bottom panel: $T \approx 68°$C

for fast prediction of the time domain input/output behavior of mildly non-linear analog circuit blocks. This model structure is able to reproduce the circuit response under non-stationary small-signal conditions, where the operating point changes dynamically during run-time. The model is cast as a reduced-order SPICE-compatible netlist, which guarantees significant speed-up in transient analyses with respect to transistor-level circuit descriptions. The efficiency of the model comes with no significant loss of accuracy, as demonstrated by several numerical experiments on voltage regulator circuit blocks.

The strong theoretical foundations of the proposed framework guarantee that the model preserves the stability properties of the reference circuit. Our main result proves in fact the quadratic stability of the LPV model, which in turn provides a guarantee of asymptotic stability for all non-stationary operating conditions belonging to the range used to construct and constrain the model.

Since the proposed framework is general, it may be extended to boost efficiency in any transient simulation scenario involving time-varying operating conditions, such as coupled electro-thermal or multiphysics simulations. These two directions will be considered in our future investigations.

Acknowledgements

References

[1] P. Toledo, R. Rubino, F. Musolino, and P. Crovetti, "Re-thinking analog integrated circuits in digital terms: A new design concept for the iot era," *IEEE Transactions on Circuits and Systems II: Express Briefs*, vol. 68, no. 3, pp. 816–822, 2021.

[2] S. Grivet-Talocia and B. Gustavsen, *Passive macromodeling: Theory and applications*. John Wiley & Sons, 2015.

[3] A. Odabasioglu, M. Celik, and L. T. Pileggi, "Prima: Passive reduced-order interconnect macromodeling algorithm," in *The Best of ICCAD*. Springer, 2003, pp. 433–450.

[4] J. R. Phillips, L. Daniel, and L. M. Silveira, "Guaranteed passive balancing transformations for model order reduction," *IEEE Transactions on Computer-Aided Design of Integrated Circuits and Systems*, vol. 22, no. 8, pp. 1027–1041, 2003.

[5] M. Sano and L. Sun, "Identification of Hammerstein-Wiener system with application to compensation for nonlinear distortion," in *41st SICE Annual Conference*, vol. 3, 2002, pp. 1521–1526.

[6] M. Rewienski and J. White, "A trajectory piecewise-linear approach to model order reduction and fast simulation of nonlinear circuits and micromachined devices," *IEEE Transactions on computer-aided design of integrated circuits and systems*, vol. 22, no. 2, pp. 155–170, 2003.

[7] J. C. Pedro and S. A. Maas, "A comparative overview of microwave and wireless power-amplifier behavioral modeling approaches," *IEEE transactions on microwave theory and techniques*, vol. 53, no. 4, pp. 1150–1163, 2005.

[8] D. E. Root, J. Verspecht, D. Sharrit, J. Wood, and A. Cognata, "Broadband poly-harmonic distortion (phd) behavioral models from fast automated simulations and large-signal vectorial network measurements," *IEEE Transactions on Microwave Theory and Techniques*, vol. 53, no. 11, pp. 3656–3664, 2005.

[9] Z. Naghibi, S. A. Sadrossadat, and S. Safari, "Time-domain modeling of nonlinear circuits using deep recurrent neural network technique," *AEU-International Journal of Electronics and Communications*, vol. 100, pp. 66–74, 2019.

[10] S. Nagaraj, D. Seshachalam, and S. Hucharaddi, "Model order reduction of nonlinear circuit using proper orthogonal decomposition and nonlinear autoregressive with exogenous input (narx) neural network," in *2018 16th ACM/IEEE International Conference on Formal Methods and Models for System Design (MEMOCODE)*. IEEE, 2018, pp. 1–4.

[11] S. Olivadese, P. Brenner, and S. Grivet-Talocia, "Dc-compliant small-signal macromodels of non-linear circuit blocks," in *2013 17th IEEE Workshop on Signal and Power Integrity*. IEEE, 2013, pp. 1–4.

[12] T. Bradde, S. Grivet-Talocia, G. C. Calafiore, A. V. Proskurnikov, Z. Mahmood, and L. Daniel, "Bounded input dissipativity of linearized circuit models," *IEEE Transactions on Circuits and Systems I: Regular Papers*, vol. 67, no. 6, pp. 2064–2077, 2020.

[13] T. Bradde, S. Grivet-Talocia, G. Calafiore, A. Proskurnikov, Z. Mahmood, and L. Daniel, "On dissipativity conditions for linearized models of locally active circuit blocks," in *IEEE 29th Conf. on Electrical Performance of Electronic Packaging and Systems*, 2020, pp. 1–3.

[14] S. B. Olivadese, G. Signorini, S. Grivet-Talocia, and P. Brenner, "Parameterized and dc-compliant small-signal macromodels of rf circuit blocks," *IEEE Transactions on Components, Packaging and Manufacturing Technology*, vol. 5, no. 4, pp. 508–522, 2015.

[15] P. Triverio, S. Grivet-Talocia, and M. S. Nakhla, "A parameterized macromodeling strategy with uniform stability test," *IEEE Transactions on Advanced Packaging*, vol. 32, no. 1, pp. 205–215, 2009.

[16] C. Briat, *Linear parameter-varying and time-delay systems*. Springer, 2014.

[17] A. Antoulas and B. Anderson, "On the scalar rational interpolation problem," *IMA Journal of Mathematical Control and Information*, vol. 3, no. 2-3, pp. 61–88, 1986.

[18] B. Gustavsen and A. Semlyen, "Rational approximation of frequency domain responses by vector fitting," *IEEE Transactions on power delivery*, vol. 14, no. 3, pp. 1052–1061, 1999.

[19] T. Bradde, P. Toledo, M. De Stefano, A. Zanco, S. Grivet-Talocia, and P. Crovetti, "Enabling fast power integrity transient analysis through parameterized small-signal macromodels," in *International Symposium on Electromagnetic Compatibility*, Barcelona, Spain, 2019, pp. 759–764.

[20] F. Ferranti, L. Knockaert, and T. Dhaene, "Parameterized s-parameter based macromodeling with guaranteed passivity," *IEEE Microwave and Wireless Components Letters*, vol. 19, no. 10, pp. 608–610, 2009.

[21] D. Deschrijver, T. Dhaene, and D. De Zutter, "Robust parametric macromodeling using multivariate orthonormal vector fitting," *IEEE Transactions on Microwave Theory and Techniques*, vol. 56, no. 7, pp. 1661–1667, 2008.

[22] A. C. Rodriguez and S. Gugercin, "The p-AAA algorithm for data driven modeling of parametric dynamical systems," *arXiv preprint arXiv:2003.06536*, 2020.

[23] P. Triverio, M. S. Nakhla, and S. Grivet-Talocia, "Parametric macromodeling of multiport networks from tabulated data," in *IEEE Electrical Performance of Electronic Packaging*. IEEE, 2007, pp. 51–54.

[24] C. Sanathanan and J. Koerner, "Transfer function synthesis as a ratio of two complex polynomials," *IEEE transactions on automatic control*, vol. 8, no. 1, pp. 56–58, 1963.

[25] B. Zhou, "On asymptotic stability of linear time-varying systems," *Automatica*, vol. 68, pp. 266–276, 2016.

[26] E. R. Samuel, L. Knockaert, F. Ferranti, and T. Dhaene, "Guaranteed passive parameterized macromodeling by using Sylvester state-space realizations," *IEEE Transactions on Microwave Theory and Techniques*, vol. 61, no. 4, pp. 1444–1454, 2013.

[27] S. Grivet-Talocia and R. Trinchero, "Behavioral, parameterized, and broadband modeling of wired interconnects with internal discontinuities," *IEEE Transactions on Electromagnetic Compatibility*, vol. 60, no. 1, pp. 77–85, 2017.

[28] A. Zanco and S. Grivet-Talocia, "High-dimensional parameterized macromodeling with guaranteed stability," in *2019 IEEE 28th Conference on Electrical Performance of Electronic Packaging and Systems (EPEPS)*. IEEE, 2019, pp. 1–3.

[29] F. Blanchini, D. Casagrande, S. Miani, and U. Viaro, "Stable LPV realization of parametric transfer functions and its application to gain-scheduling control design," *IEEE Transactions on Automatic Control*, vol. 55, no. 10, pp. 2271–2281, 2010.

[30] W. J. Rugh and J. S. Shamma, "Research on gain scheduling," *Automatica*, vol. 36, no. 10, pp. 1401–1425, 2000.

[31] X. Zhang, P. Tsiotras, and C. Knospe, "Stability analysis of LPV time-delayed systems," *International journal of control*, vol. 75, no. 7, pp. 538–558, 2002.

[32] P. Gahinet, P. Apkarian, and M. Chilali, "Affine parameter-dependent Lyapunov functions and real parametric uncertainty," *IEEE Transactions on Automatic control*, vol. 41, no. 3, pp. 436–442, 1996.

[33] J. S. Shamma, "An overview of LPV systems," *Control of linear parameter varying systems with applications*, pp. 3–26, 2012.

[34] T. Bradde, S. Grivet-Talocia, M. De Stefano, and A. Zanco, "A scalable reduced-order modeling algorithm for the construction of parameterized interconnect macromodels from scattering responses," in *2018 IEEE Symposium on Electromagnetic Compatibility, Signal Integrity and Power Integrity (EMC, SI & PI)*. IEEE, 2018, pp. 650–655.

[35] G. G. Lorentz, *Bernstein polynomials*. Amer. Math. Soc., 2013.

[36] S. Grivet-Talocia, "On driving non-passive macromodels to instability," *International Journal of Circuit Theory and Applications*, vol. 37, no. 8, pp. 863–886, 2009.

[37] R. E. Kalman, "Lyapunov functions for the problem of Lur'e in automatic control," *Proceedings of the National Academy of Sciences of the United States of America*, vol. 49, no. 2, p. 201, 1963.

[38] J. De Caigny, R. Pintelon, J. F. Camino, and J. Swevers, "Interpolated modeling of LPV systems," *IEEE Transactions on Control Systems Technology*, vol. 22, no. 6, pp. 2232–2246, 2014.

[39] D. Vizer, G. Mercere, O. Prot, and J. Ramos, "A local approach framework for black-box and gray-box LPV system identification," in *European Control Conference (ECC)*, 2013, pp. 1916–1921.

[40] Z. Alkhoury, M. Petreczky, and G. Mercère, "Comparing global input-output behavior of frozen-equivalent LPV state-space models," *IFAC-PapersOnLine*, vol. 50, no. 1, pp. 9766–9771, 2017.

[41] R. J. Milliken, J. Silva-Martínez, and E. Sánchez-Sinencio, "Full on-chip cmos low-dropout voltage regulator," *IEEE Transactions on Circuits and Systems I: Regular Papers*, vol. 54, no. 9, pp. 1879–1890, 2007.

[42] T. Y. Man, P. K. Mok, and M. Chan, "A high slew-rate push–pull output amplifier for low-quiescent current low-dropout regulators with transient-response improvement," *IEEE Transactions on Circuits and Systems II: Express Briefs*, vol. 54, no. 9, pp. 755–759, 2007.

[43] P. Minh, "Diamond/CNT film interface for heat dissipation in electronic devices," *Report of Asian Office of Aerospace Research and Development*, p. 10, 09 2009.

Tommaso Bradde received the Bachelor degree in Electronic Engineering from Roma Tre University, Rome, Italy, in 2015 and the master degree in Mechatronic Engineering at Politecnico di Torino, Turin, Italy, in 2018. He is currently a third-year Ph.D. student in Electrical, Electronics and Communication Engineering within the Politecnico di Torino. His current research is focused on data-driven parameterized macromodeling and its applications to system level signal and power integrity assesments, with the inclusion of active devices.

Stefano Grivet-Talocia (M'98–SM'07–F'18) received the Laurea and Ph.D. degrees in electronic engineering from the Politecnico di Torino, Turin, Italy. From 1994 to 1996, he was with the NASA/Goddard Space Flight Center, Greenbelt, MD, USA. He is currently a Full Professor of electrical engineering with the Politecnico di Torino. He co-founded the academic spinoff company IdemWorks in 2007, serving as the President until its acquisition by CST in 2016. He has authored about 200 journal and conference papers. His current research interests include passive macromodeling of lumped and distributed interconnect structures, model-order reduction, modeling and simulation of fields, circuits, and their interaction, wavelets, time-frequency transforms, and their applications. Dr. Grivet-Talocia was a co-recipient of the 2007 Best Paper Award of the IEEE TRANSACTIONS ON ADVANCED PACKAGING. He received the IBM Shared University Research Award in 2007, 2008, and 2009. He was an Associate Editor of the IEEE TRANSACTIONS ON ELECTROMAGNETIC COMPATIBILITY from 1999 to 2001 and He is currently serving as Associate Editor for the IEEE TRANSACTIONS ON COMPONENTS, PACKAGING AND MANUFACTURING TECHNOLOGY. He was the General Chair of the 20th and 21st IEEE Workshops on Signal and Power Integrity (SPI2016 and SPI2017).

Pedro Toledo (Graduate Student Member, IEEE) received the B.Sc. degree in electronic engineering from the Universidade Federal de Pernambuco (UFPE), Recife, Brazil, in 2010, and the M.Sc. degree in microelectronics from the Universidade Federal do Rio Grande do Sul (UFRGS), Porto Alegre, Brazil, in 2015. He completed the IC-Brazil Program in 2011. Since 2018 he is a Ph.D. student at Politecnico di Torino, and UFRGS (Joint-Degree Ph.D.) working with digital-based analog processing for IoT applications.

Anton Proskurnikov (M'13, SM'18) is an Assistant Professor at the Department of Electronics and Telecommunications, Politecnico di Torino (Italy). He received the M.Sc. (2003) and Ph.D. (2005) degrees from St. Petersburg State University. He was an assistant professor and senior researcher at St. Petersburg State University (2003-2010), and later a postdoctoral researcher at the University of Groningen (2014-2016) and TU Delft (2016-2018). His research interests include nonlinear dynamics, complex networks, robust and nonlinear control.

Alessandro Zanco received the Bachelor Degree in Electrical Engineering in 2015 and the Master degree in Mechatronic Engineering in 2018 from Politecnico di Torino, Torino, Italy. He is currently pursuing his Ph.D in Electrical, Electronics and Communication Engineering, at Politecnico di Torino. His research interests include high-dimensional parameterized black-box modeling for EMC.

Giuseppe Calafiore is a full professor at DET, Politecnico di Torino, where he coordinates the Systems and Data Science group, and an associate fellow of the IEIIT-CNR. Dr. Calafiore held several visiting positions at international institutions: at the Information Systems Laboratory (ISL), Stanford University, California, in 1995; at the Ecole Nationale Supérieure de Techniques Avancées (EN-STA), Paris, in 1998; and at the University of California at Berkeley, in 1999, 2003, 2007, 2017 and 2018. He was a Senior Fellow at the Institute of Pure and Applied Mathematics (IPAM), University of California at Los Angeles, in 2010. Dr. Calafiore is the author of more than 190 journal and conference proceedings papers, and of eight books. He is a Fellow of the IEEE. He received the IEEE Control System Society "George S. Axelby" Outstanding Paper Award in 2008. His research interests are in the fields of convex optimization, randomized algorithms, identification, and control of uncertain systems, with applications ranging from finance and economic systems to robust control, machine learning, and data science.

Paolo Crovetti (Senior Member, IEEE) was born in Turin, Italy, in 1976. He received the Laurea degree (summa cum laude) and the Ph.D. degree in electronic engineering from the Politecnico di Turin, Turin, in 2000 and 2003, respectively. He is currently an Associate Professor with the Department of Electronics and Telecommunications (DET), Politecnico di Torino, Turin. He has co-authored more than 80 articles appearing in journals and international conference proceedings. His main research interests are in the field of analog and mixed-signal IC design and IC-level and system-level electromagnetic compatibility. His recent research activities are focused on non-conventional information processing techniques allowing the fully digital implementations of analog functions and on the effects of spread-spectrum modulations on digital data lines. Prof. Crovetti is the Subject Editor-in-Chief of IET Electronics Letters in the area of Circuits and Systems and is an Associate Editor of the IEEE TRANSACTIONS ON VERY LARGE SCALE INTEGRATION SYSTEMS. He serves as a regular reviewer for several IEEE journals.